

Microscopic mechanisms of thermal and driven diffusion of non rigid molecules on surfaces

C. Fusco* and A. Fasolino

Department of Theoretical Physics, University of Nijmegen, Toernooiveld 1, 6525 ED Nijmegen, The Netherlands

The motion of molecules on solid surfaces is of interest for technological applications such as catalysis and lubrication, but it is also a theoretical challenge at a more fundamental level. The concept of activation barriers is very convenient for the interpretation of experiments and as input for Monte Carlo simulations but may become inadequate when mismatch with the substrate and molecular vibrations are considered. We study the simplest objects diffusing on a substrate at finite temperature T , namely an adatom and a diatomic molecule (dimer), using the Langevin approach. In the driven case, we analyse the characteristic curves, comparing the motion for different values of the intramolecular spacing, both for $T = 0$ and $T \neq 0$. The mobility of the dimer is higher than that of the monomer when the drift velocity is less than the natural stretching frequency. The role of intramolecular excitations is crucial in this respect. In the undriven case, the diffusive dynamics is considered as a function of temperature. Contrary to atomic diffusion, for the dimer it is not possible to define a single, temperature independent, activation barrier. Our results suggest that vibrations can account for drastic variations of the activation barrier. This reveals a complex behaviour determined by the interplay between vibrations and a temperature dependent intramolecular equilibrium length.

I. INTRODUCTION

The diffusion of adatoms and molecules on surfaces is recently attracting much attention, in order to understand many properties of technological interest, such as thin film growth, catalysis and dissociation [1,2]. Useful experimental techniques for probing the surface diffusion of molecular adsorbates have been developed. These allow to follow the dynamical details of surface diffusion, using Scanning Tunneling Microscopy [3], and to image physisorbed atoms and clusters, using Field Ion Microscopy [4]. Most theoretical works have focussed on the determination of energy barriers for diffusion in different systems [5–9], usually on the basis of energy arguments and neglecting the role of internal degrees of freedom. However, it is often suggested that diffusion dynamics can be strongly affected by the presence of intramolecular motion [10,11]. Here we address this problem for the simple but important case of a dimer physisorbed on a periodic substrate, trying to link the macroscopic diffusive behaviour to microscopic degrees of freedom. Our theoretical model contains the salient features of a diatomic molecule physisorbed on a periodic substrate. However, our work does not aim to probe diffusion in a specific molecule-surface system, but to understand diffusion mechanisms expected for systems of this kind.

In Sec. II we give some details of the model we have used. Sec. III is devoted to the discussion of the results in the presence of an external driving, while Sec. IV deals with pure thermal diffusion. Some concluding remarks are presented in the last section.

II. MODEL

We consider a monomer (adatom) and a dimer (diatomic molecule) moving on a periodic one-dimensional substrate at finite temperature. The particle-substrate interaction is modelled by a periodic function U . Specifically, for the monomer

$$U(x) = U_0(1 - \cos(kx)) \quad (1)$$

and for the dimer

$$U(x_1, x_2) = U_0(2 - \cos(kx_1) - \cos(kx_2)), \quad (2)$$

where x represents the spatial coordinate and $k = 2\pi/a$, a being the lattice constant of the substrate.

For the dimer the interparticle interaction is taken to be harmonic:

$$V(x_1, x_2) = \frac{K}{2}(x_2 - x_1 - l)^2, \quad (3)$$

where l is the spring equilibrium length. In order to take into account the finite temperature T of the substrate, we adopt the Langevin approach. In this framework the motion of the sliding object is described exactly, while the substrate is treated as a thermal bath. The equations of motion of the monomer and the dimer are respectively

$$m\ddot{x} + m\eta\dot{x} = -U_0 \sin(kx) + f + F \quad (4)$$

*Author to whom correspondence should be addressed. Electronic address: fusco@sci.kun.nl.

and

$$\begin{cases} m\ddot{x}_1 + m\eta\dot{x}_1 = K(x_2 - x_1 - l) - U_0 \sin(kx_1) + f_1 + F \\ m\ddot{x}_2 + m\eta\dot{x}_2 = K(x_1 - x_2 + l) - U_0 \sin(kx_2) + f_2 + F, \end{cases} \quad (5)$$

where an explicit damping term $m\eta\dot{x}_i$ modelling energy dissipation has been introduced (η is the phenomenological friction coefficient), and the effect of finite temperature T is taken into account by the stochastically fluctuating forces f_i . These two terms are related by the dissipation-fluctuation theorem:

$$\langle f_i(t)f_j(0) \rangle = 2mk_B T \delta_{ij} \delta(t). \quad (6)$$

It is convenient to rewrite the equation of motion in adimensional units by introducing a characteristic time

$$\tau = \left(\frac{m}{k_B T k^2} \right)^{1/2}$$

and defining

$$\tilde{x} = kx, \quad \tilde{t} = t/\tau, \quad \tilde{\eta} = \eta\tau, \quad \tilde{U}_0 = U_0/(k_B T)$$

$$\tilde{f} = f/(kk_B T), \quad \tilde{F} = F/(kk_B T), \quad \tilde{l} = kl, \quad \tilde{K} = K/(k^2 k_B T).$$

For typical values $m \sim 2 \cdot 10^{-26} \text{Kg}$, $T = 300\text{K}$, $a \sim 2\text{\AA}$, we have $\tau \simeq 0.25\text{ps}$. In this way Eqs. (4) and (5) become (in the following we omit the tildes for simplicity)

$$\ddot{x} + \eta\dot{x} = -U_0 \sin x + f + F \quad (7)$$

and

$$\begin{cases} \ddot{x}_1 + \eta\dot{x}_1 = K(x_2 - x_1 - l) - U_0 \sin x_1 + f_1 + F \\ \ddot{x}_2 + \eta\dot{x}_2 = K(x_1 - x_2 + l) - U_0 \sin x_2 + f_2 + F, \end{cases} \quad (8)$$

and the fluctuation-dissipation relation Eq. (6)

$$\langle f_i(t)f_j(0) \rangle = 2\eta\delta_{ij}\delta(t). \quad (9)$$

We perform Molecular Dynamics (MD) simulations, integrating the equations of motion using a velocity-Verlet algorithm, with time step $\Delta = 10^{-4}\tau$, averaging the trajectories over several hundreds of realizations ($\simeq 300$ in driven case and $\simeq 3000$ in the undriven case with $F = 0$), in order to reduce the statistical noise due to the stochastic term.

III. DRIVEN CASE

We have analyzed the response properties of Eqs. (7) and (8) by studying the characteristic curves, i.e. the behaviour of the mobility of the system subjected to the

external force F . For the monomer, we can rely on the results of Kramers' Transition State Theory (TST) [12–14], yielding analytical results for certain regimes of friction and for relatively high values of the diffusion barrier $2U_0$. We present in Fig. 1 the results obtained with our simulation for $U_0 = 2.5$ and $\eta = 1$, which we will use as reference in discussing the behaviour of the dimer. Fig. 1(a) shows the velocity-force characteristic in the $T = 0$ case. Increasing F adiabatically the velocity remains zero until a critical force F_1^{mon} is reached, since the system has to overcome a finite static friction force in order to get out of the potential well. Then the particle slides with constant velocity v on the substrate, resulting in a linear relation between v and F for high values of the driving force:

$$F \simeq \eta v. \quad (10)$$

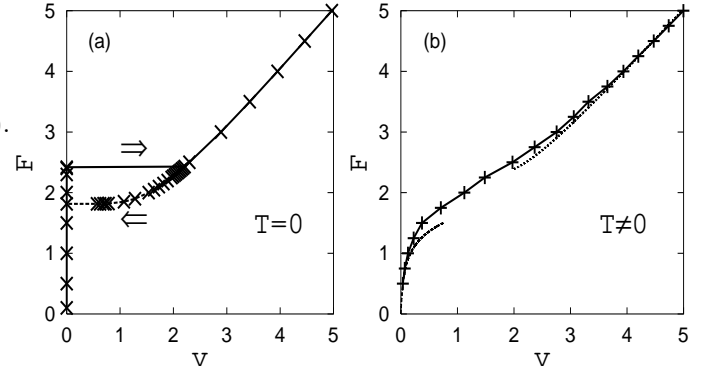


FIG. 1. Characteristic curve of the monomer for $T = 0$ (a) and $T \neq 0$ (b). The arrows in (a) indicate the parts of the curve where the force is increased or decreased. The lines with crosses in (a) and (b) are the numerical data, while the dashed line and the dotted line in (b) are fits to the data respectively according to Eq. (11) and Eq. (12). The parameters used are $U_0 = 2.5$ and $\eta = 1$.

If we decrease the force adiabatically a hysteresis effect is observed, since the mobility is different from zero also when $F < F_1^{mon}$ and vanishes at $F = F_2^{mon} < F_1^{mon}$. This corresponds to a bistability between the locked and the running solution, which is present when the friction coefficient η is not very large, $\eta/\sqrt{U_0} < 1.19$ [14]. In the case $T \neq 0$ this bistability disappears, at least for intermediate-large values of η . The system has always the chance to get untrapped because of thermal fluctuations. As a consequence the mobility is always different from zero when $F \neq 0$, as shown in Fig. 1(b). If η is relatively large, it is possible to describe analytically the behaviour for small F by means of Kramers' TST [12]. The result for the behaviour of $v(F)$ is

$$v = \left\{ \left[\frac{\eta^2}{4} + U_0 \cos \left(\arcsin \left(\frac{F}{U_0} \right) \right) \right]^{1/2} - \frac{\eta}{2} \right\} \times \exp(-2U_0) (\exp(Fa/2) - \exp(-Fa/2)) \quad (11)$$

As we can see from Fig. 1(b), Eq. (11) reproduces the simulation results for $F < 1$, but this range increases for larger values of U_0 , where the activated processes are more pronounced. The behaviour of the mobility for large F , where the particle performs a drift motion with a small contribution of the noise term can be shown to be [15]

$$F = \eta v \left(1 + \frac{U_0^2}{2v^4} \right). \quad (12)$$

In particular, if F is very large compared to U_0 the term in parenthesis tends to one and the characteristic curve becomes linear:

$$F \simeq \eta v. \quad (13)$$

Now we consider the driven dimer described by Eq. (8). In this case, the presence of the interparticle interaction renders the problem more complex, giving rise to a richer dynamical behaviour. We have analyzed the characteristic curves for different values of the intramolecular spacing l , namely $l = a$, $l = a/2$ and $l = \tau_g a$ where $\tau_g = (1 + \sqrt{5})/2$ is the golden mean, both for $T = 0$ and $T \neq 0$ (see Fig. 2), and compared them to the monomer characteristics (see Fig. 3).

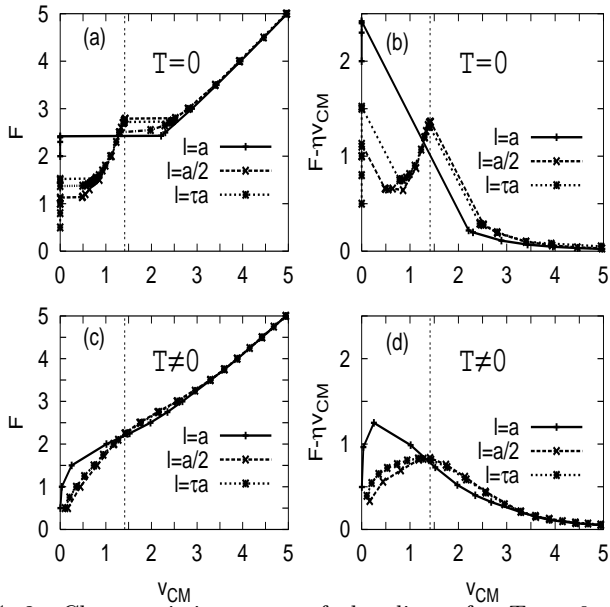


FIG. 2. Characteristic curves of the dimer for $T = 0$ (a),(b) and $T \neq 0$ (c),(d) for three values of l . The vertical dot-dashed line passes through $v_{CM} = \omega_0$. The parameters used are $U_0 = 2.5$, $\eta = 1$ and $K = 1$.

Note that we have chosen $l = \tau_g a$ because it is a prototypical example of an incommensurate length ratio.

For the dimer it is convenient to rewrite the equation of motion using the centre of mass (CM) and relative coordinates, defined by

$$x_{CM} = (x_1 + x_2)/2 \quad y_r = x_2 - x_1 - l. \quad (14)$$

From Eq. (8) we obtain

$$\begin{cases} \ddot{x}_{CM} = -\eta \dot{x}_{CM} - U_0 \cos((y_r + l)/2) \sin x_{CM} + F \\ \ddot{y}_r = -\eta \dot{y}_r - 2K y_r - 2U_0 \sin((y_r + l)/2) \cos x_{CM} \end{cases} \quad (15)$$

In our MD simulations we choose the initial configuration which minimizes the total potential energy. As for the monomer a critical force F_1^{dim} , which depends on the value of l , is needed to achieve motion for $T = 0$. Then for larger values of F the velocity increases as a function of the external force, but at a certain value of the force F_3^{dim} another plateau appears in the $v_{CM} - F$ plane (v_{CM} being the CM mean velocity), signalling a dynamical crossover in the system. Finally, keeping on increasing the force, the linear regime is recovered (Fig. 2(a)). In the CM frame, the external potential leads, for a drift motion $x_{CM} \sim v_{CM} t$, to a time-periodic force acting on the particles, with “washboard” frequency given by v_{CM} .

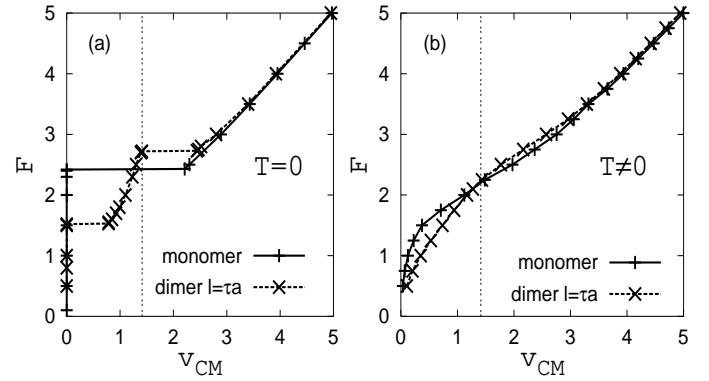


FIG. 3. Comparison between the characteristic curves of the monomer and the dimer for $T = 0$ (a) and $T \neq 0$ (b). The parameters used are the same as in Figs. 1 and 2.

The force F_3^{dim} , where the second plateau appears, physically corresponds to the point where the washboard frequency is in resonance with the stretching frequency of the dimer $\omega_0 = (2K)^{1/2}$, exciting the internal degrees of freedom. This resonance mechanism was also found in the Frenkel-Kontorova model in the low friction limit [16]. For the dimer two regions of bistability can be observed, corresponding to the two plateaus in the characteristic curve; thus, when F is decreased a first hysteresis occurs in proximity of $v_{CM} = \omega_0$, giving a critical value

$F_4^{dim} < F_3^{dim}$, where the characteristic curve has a discontinuous derivative, while a second hysteresis is found when F is decreased further from F_1^{dim} and another critical value $F_2^{dim} < F_1^{dim}$, where $v_{CM} = 0$, is obtained as for the monomer (these hysteresis curves are shown only for the $l = \tau_g a$ dimer in Fig. 2). For a closer comparison between the monomer and the dimer at $T = 0$ see Fig. 3(a). We note that the qualitative behaviour is the same for different l but the values of F_1^{dim} and F_2^{dim} can differ significantly as a function of l . This is due to energetic reasons: the dimer with $l = a/2$ is energetically favourite since, on average, it has to overcome a lower barrier, while for $l = a$ the two particles tend to be pinned in the minima and to behave like a monomer (in fact the characteristic curve of the $l = a$ dimer is practically superimposed on that of the monomer). The resonance frequency is highlighted in Fig. 2(b) by plotting $F - \eta v_{CM}$ as a function of v_{CM} : a clear peak of the characteristic curves at $v_{CM} = \omega_0$ is visible when $l \neq a$.

In order to understand better the resonance mechanisms we consider the case $l = a$ at $T = 0$. Assuming a CM drift motion, $x_{CM}(t) = x_0 + v_{CM}t$, and linearizing the equation of motion (15) for $l = a$ we obtain the following equation for y_r :

$$\ddot{y}_r + \eta \dot{y}_r + 2K y_r = U_0 \cos(v_{CM}t + x_0) y_r. \quad (16)$$

This is the equation of a parametric oscillator, for which an exponential increase of the amplitude is expected for $v_{CM} \simeq 2\omega_0$ within a given instability window, which we estimate to be $2.21 < v_{CM} < 2.37$. We note that indeed the amplitude of y_r increases exponentially in a certain range of F , as shown in Fig. 4, but it saturates at long times. This is due to the fact that Eq. (16) assumes a constant CM velocity. Actually, in the full system Eq. (15) x_{CM} is coupled to y_r , so that v_{CM} decreases slightly during the dynamics as shown in Fig. 4(d). This is enough to shift v_{CM} out of the instability window, thus stopping the increase of y_r .

This shows how intramolecular vibrations can be resonantly excited due to the sliding on a periodic substrate and that the details of the resulting relative motion are non trivial. For instance, whether this could represent a mechanism for dissociation depends on the maximum excursion from the equilibrium distance. Moreover, the very nature of parametric resonances makes the temporal behaviour very much dependent on the initial values of the interatomic spacing which is in turn related to vibrational energy and temperature.

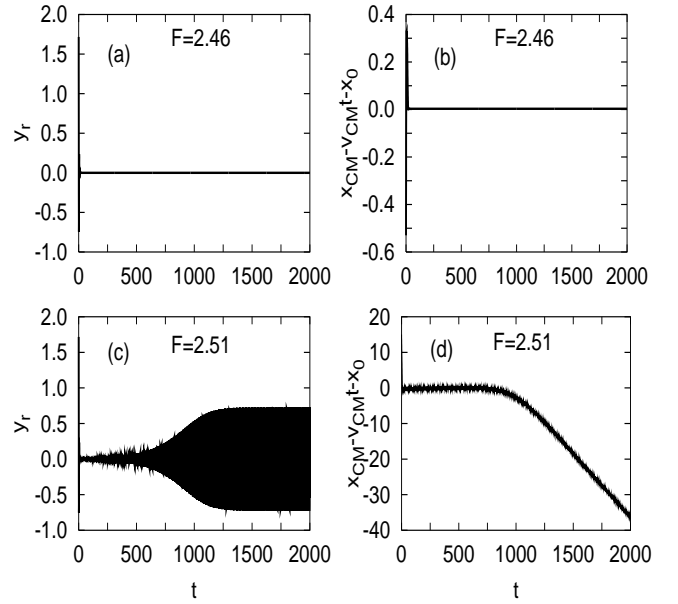


FIG. 4. Relative and CM motion of the dimer for $l = a$ with initial condition $x_2 - x_1 = 1.27a$, for different values of the external driving F . y_r is shown in (a) and (c), while the deviation of $x_{CM} - x_0$ from $v_{CM}t$ is plotted in (b) and (d) (x_0 is the initial condition for CM). The parameters used are the same as in Fig. 2.

The behaviour outlined for $T = 0$ smears out at finite temperatures. Although a hysteretic behaviour has been found for long periodic chains in the low friction limit [17], no bistabilities and hysteresis are present in our case, as shown in Fig. 2(c). The static friction force vanishes and the mobility is sensitive to the value of l . In particular the dimer with $l = a$ has the lowest mobility. Note that the curves for different l still cross at $v_{CM} = \omega_0$. This crossover of the mobility can be observed also comparing the monomer and the dimer (Fig. 3(b)). Moreover, as it can be seen from Fig. 2(d), plotting $F - \eta v_{CM}$ vs. v_{CM} , the resonance peak at $v_{CM} = \omega_0$ still survives for $l \neq a$. For $l = a$ the peak is shifted to a smaller value of v_{CM} . This is due to the fact that in the commensurate case, even though the static friction force found at $T = 0$ vanishes, a larger force is needed to reach the sliding state and this corresponds to the point of highest curvature in the characteristic plotted in Fig. 2(c). To a certain extent this resembles the monomer case, where a very similar behaviour is found.

IV. DIFFUSION

Next we examine the pure thermal diffusion, i.e. we study the motion of the monomer and the dimer with $F = 0$. This problem is computationally more time consuming, since the motion is completely random and an averaging over many MD realizations is needed. We extract information about the diffusive behaviour of the particles by computing the Mean Square Displacement

(MSD) $\langle x^2(t) \rangle$, where $\langle \cdot \rangle$ denotes the average over the realizations. The diffusion coefficient D is defined by

$$D = \lim_{t \rightarrow \infty} \frac{\langle x^2(t) \rangle}{2t}. \quad (17)$$

Usually it is assumed that the dependence of D on temperature should follow the Arrhenius law:

$$D = D_0 \exp(-E_a) \quad (18)$$

where D_0 is a prefactor and E_a is the activation energy for diffusion, scaled to $k_B T$. In Eq. (18) both D_0 and E_a are assumed to be T independent. However, some recent studies have already shown that there may be deviations from the Arrhenius behaviour [10,11,18]. Fig. 5 shows the diffusion coefficient D as a function of the single-particle energy barrier $E_b = 2U_0$ (scaled to $k_B T$) for the monomer and the dimer for different values of l and two values of K . We note that while the monomer has a uniquely defined activation energy $E_a \simeq 0.95$, a clear deviation from the Arrhenius law is observed in the dimer case, except for the case $l = a$, where it is less evident (as explained in Sec. III the commensurate dimer dynamics is similar to that of the monomer).

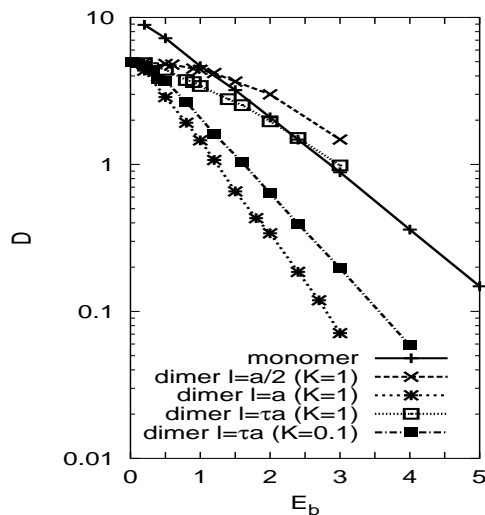


FIG. 5. Diffusion coefficient of the monomer and the dimer for different values of l and K vs. $E_b = 2U_0$. Here $F = 0$ and $\eta = 0.1$. Note that for the free diffusion case $E_b \rightarrow 0$ the diffusion coefficient of the monomer is $\frac{1}{\eta} = 10$ while that of the dimer is $\frac{1}{2\eta} = 5$ (independent of l).

The $l = a/2$ dimer diffuses faster than the monomer (at least for $E_b > 1$) due to the most favourable energy configuration (see also [6]). Note that the crossover point in the diffusion behaviour can depend on the force constant K , as it can be seen by comparing the two curves for $l = \tau_a a$ with $K = 1$ and $K = 0.1$. The dependence of the activation energy on temperature (or equivalently on the energy barrier) can be attributed to a temperature dependent intramolecular length, which affects the diffusion behaviour especially in the high temperature regime

(low E_b). A similar mechanism was also proposed in a model of heteroepitaxial island diffusion [11]. Since we are considering small values of E_b (rigorously Eq. (18) should be valid for $E_b \rightarrow \infty$), finite-barrier effects are also important, as illustrated in Ref. [18]. We are currently trying to unravel the latter from the effects due to vibrations. Our results suggest that the role of intramolecular vibrations is relevant for the diffusion dynamics. The possibility to excite internal degrees of freedom, even for a simple diatomic molecule, can affect the temperature dependence of the activation energy [10] and determine a complex diffusion behaviour which can depend on the lattice commensurability and on the interatomic spacing. We plan to address this issue more extensively in a future work.

V. CONCLUSIONS AND PERSPECTIVES

We have presented a simplified model to study the driven and undriven motion of monomers and dimers on a periodic substrate. We have pointed out the peculiar effects of the substrate on the CM and relative motion of the dimer, such as nonlinear mobility, bistabilities and resonance processes. In this respect, the coupling between the internal degrees of freedom is crucial. In particular, the diffusion dynamics reveals strikingly complex features determined both by energetic mechanisms and by the role of intramolecular motion. It would be worthwhile to explore further this issue going from the simple 1D model to a more realistic approach, considering for example the motion and the orientation of large molecules on a 2D surface and the diffusion of long chains.

ACKNOWLEDGMENTS

This work was supported by the Stichting Fundamenteel Onderzoek der Materie (FOM) with financial support from the Nederlandse Organisatie voor Wetenschappelijk Onderzoek (NWO).

-
- [1] R. Gomer, Rep. Prog. Phys. 53, 917 (1990).
 - [2] G. L. Kellogg, Surf. Sci. Rep. 21, 1 (1994).
 - [3] E. Ganz, S. K. Theiss, I. Hwang, J. Golovchenko, Phys. Rev. Lett. 68, 1567 (1992).
 - [4] G. L. Kellogg, Phys. Rev. Lett. 67, 216 (1991).
 - [5] J. S. Raut, K. A. Fichthorn, J. Chem. Phys. 108, 1626 (1998).
 - [6] D. S. Sholl, K. A. Fichthorn, Phys. Rev. Lett. 79, 3569 (1997).

- [7] T. R. Linderoth, S. Horch, E. Laegsgaard, I. Stensgaard, F. Besenbacher, *Surf. Sci.* 402, 308 (1998).
- [8] M. Schunack, T. R. Linderoth, F. Rosei, E. Laegsgaard, I. Stensgaard, F. Besenbacher, *Phys. Rev. Lett.* 88, 156102 (2002).
- [9] G. Boisvert, L. J. Lewis, *Phys. Rev. B* 56, 7643 (1997).
- [10] S. Yu. Krylov, L. J. F. Hermans, *Phys. Rev. B*, 092205 (2002).
- [11] J. C. Hamilton, *Phys. Rev. Lett.* 77, 885 (1996).
- [12] H.A. Kramers, *Physica* 7, 284 (1940).
- [13] P. Hänggi, P. Talkner, M. Borkovec, *Rev. Mod. Phys.* 62, 251 (1990).
- [14] H. Risken, *The Fokker-Planck Equation*, 2nd ed., Springer, chap. 11 (1989).
- [15] B. N. J. Persson, *Phys. Rev. B* 48, 18140 (1993).
- [16] T. Strunz, F.-J. Elmer, *Phys. Rev. E* 58, 1601 (1998).
- [17] O. M. Braun, T. Dauxois, M.V. Paliy, M. Peyrard, *Phys. Rev. E* 55, 3598 (1997).
- [18] F. Montalenti, R. Ferrando, *Phys. Rev. B* 59, 5881 (1999).